Section A-Research paper
ISSN 2063-5346

Research Article

Febrifugine and Glycosminine as potential VEGFR-2 Kinase inhibitors for the treatment of Cancer: In depth in silico exploration

Rita D. Chakole[1*], Manoj S. Charde[1], Nilima N. Khakal[2], Indrajeet D. Gonjari[1]

[1]Government College of Pharmacy, Vidyanagar, Karad, Satara 415124, Maharashtra, India;
[2]Late Advocate Dadasaheb Chavan Memorial Institute of Pharmacy Malwadi, Masur. Karad, Satara (MS), India.

Corresponding author email: kdcritu@gmail.com

Abstract

Febrifugine and Glycosminine, a quinazolinone alkaloid, was initially discovered in the Chinese herb *Dichroa febrifuga*. These Vascular Endothelial Growth Factor Receptor-2 (VEGFR-2) kinase inhibitors have been found to effectively suppress the process of angiogenesis or lymphangiogenesis, thereby exhibiting notable anticancer properties. In the current study, we have chosen two naturally occurring compounds, Febrifugine and Glycosminine, as the focus of investigation. The objective is to assess their potential as inhibitors of VEGFR-2 kinase activity. In depth ADMET analysis of these compounds were done to assess their drug-likeness properties. Fro *in silico* ADMET analysis it was concluded that these compounds possess most favorable drug-likeness properties and can be treated as lead molecules for further analysis by molecular docking. From molecular docking it was observed that both the compounds formed more stable complex than native ligand. Both the compounds displayed formation of 2-3 conventional hydrogen bonds which indicates they has potential to modulate the activity of target enzyme. These compounds can be tested further using *in vitro* and *in vivo* models for VEGFR-2 kinase activity.

Keywords: VEGFR-2; Febrifugine; Glycosminine; ADMET; Cancer

1. Introduction

VEGFR-2, also known as vascular endothelial growth factor receptor 2, is a glycoprotein with a molecular weight ranging from 210 to 230 kilodaltons. It is primarily found in vascular endothelial cells and hematopoietic stem cells. VEGFR-2 plays a crucial role in mediating the cellular responses to vascular endothelial growth factor A (VEGF-A) by binding to this specific ligand. VEGFR-2 exhibits a close relationship with VEGFR-1 due to the presence of shared ligands as well as distinct ligands. However, it is noteworthy that VEGFR-2 displays a significantly heightened level of kinase activity, whereas VEGFR-1 functions as a receptor tyrosine kinase with impaired activity[1,2]. The aforementioned receptor serves as a pivotal

regulator in the modulation of responses within the endothelial cells, specifically in relation to vascular endothelial growth factor (VEGF). The aforementioned regulations encompass the aspects of permeability, proliferation, invasion, and migration. The autophosphorylation sites Y1175 and Y1214 have been identified as the primary signaling pathways associated with the human Vascular Endothelial Growth Factor Receptor 2 (VEGFR-2) upon binding with VEGF. The activation of various downstream pathways is contingent upon the autophosphorylation of Vascular Endothelial Growth Factor Receptor 2 (VEGFR-2). This crucial event is observed to be hyperactivated in certain tumor types. The aforementioned signaling pathways play a crucial role in the process of tumor angiogenesis, a phenomenon that promotes tumor proliferation through the provision of oxygen and essential nutrients to the tumor mass. The overexpression of VEGFR-2 has been observed in various types of cancers, including ovarian, thyroid, melanoma, and medulloblastoma[3–6].

VEGFR-2 inhibitors, alternatively referred to as kinase insert domain receptor (KDR) inhibitors, are a class of compounds that specifically target and inhibit the activity of the tyrosine kinase receptor known as VEGFR-2. These inhibitors have been found to effectively suppress the process of angiogenesis or lymphangiogenesis, thereby exhibiting notable anticancer properties. Typically, these compounds are diminutive, artificially produced entities that exhibit competitive binding affinity towards the adenosine triphosphate (ATP)-binding site within the tyrosine kinase domain. The interruption of multiple signaling pathways involved in tumor, such as proliferation, metastasis, and angiogenesis, can be achieved through the use of a VEGFR-2 selective inhibitor[7,8].

Febrifugine and Glycosminine, a quinazolinone alkaloid, was initially discovered in the Chinese herb *Dichroa febrifuga*. However, subsequent research has revealed its presence in the garden plant Hydrangea as well. Febrifugine, a naturally occurring compound, exhibits notable antimalarial properties. Its synthetic halogenated derivative, halofuginone, has been employed in veterinary medicine as a coccidiostat, a substance used to combat coccidiosis in animals. Various synthetic derivatives of febrifugine have been employed in the treatment of malaria, cancer, fibrosis, and inflammatory conditions, among others[9–11]. In the current study, we have chosen two naturally occurring compounds, Febrifugine and Glycosminine, as the focus of investigation. The objective is to assess their potential as inhibitors of Vascular Endothelial Growth Factor Receptor-2 (VEGFR-2) kinase activity.

2. Material and Methods

2.1 Pharmacokinetics predictions

The Lipinski rule of five and the pharmacokinetic (ADME) characteristics of molecules were investigated using PubChem[12], molinspiration[13], and SwissADME[14] servers. ADMETlab 2.0 is a totally revamped version of the AMDETlab web server, which is commonly used for predicting

the pharmacokinetics and toxic characteristics of various compounds (https://admetmesh.scbdd.com/)[15].

2.2 Molecular docking studies

Molecular docking is a fundamental aspect of computer-assisted drug discovery and structural molecular biology. Using a method known as "ligand-protein docking," scientists may foretell how a ligand will interact with a protein whose three-dimensional structure is already known. A precise scoring system for dockings in high-dimensional areas is essential. One may do virtual screening on a large library of compounds, grade the results, and propose structural ideas of how the ligands block the target, which is highly valuable in lead optimization[16–20].

In order to achieve further optimization, the molecules underwent binding affinity studies with the target enzyme. All the selected compounds and the native ligand were docked against the Crystal structure of the KDR (VEGFR2) kinase domain in complex with a type-II inhibitor bearing an acrylamide using Autodock vina 1.1.2 in PyRx 0.8[21]. ChemDraw Ultra 8.0 was used to draw the structures of the compounds and native ligand (mole. File format). All the ligands were subjected for energy minimization by applying Universal Force Field (UFF)[22]. The crystal structure of the enzyme with PDB ID: 6XVK was obtained from RCSB Protein Data Bank (PDB) (https://www.rcsb.org/structure/6XVK). Discovery Studio Visualizer (version-19.1.0.18287) was used to refine the enzyme structure, purify it, and get it ready for docking[23]. A three-dimensional grid box with an exhaustiveness value of 8 was created for molecular docking[21]. BIOVIA Discovery Studio Visualizer was used to locate the protein's active amino acid residues. The approach outlined by Khan et al. was used to perform the entire molecular docking procedure, identify cavity and active amino acid residues[24–30]. Fig. 1 shows the revealed cavity of enzyme with the native ligand.

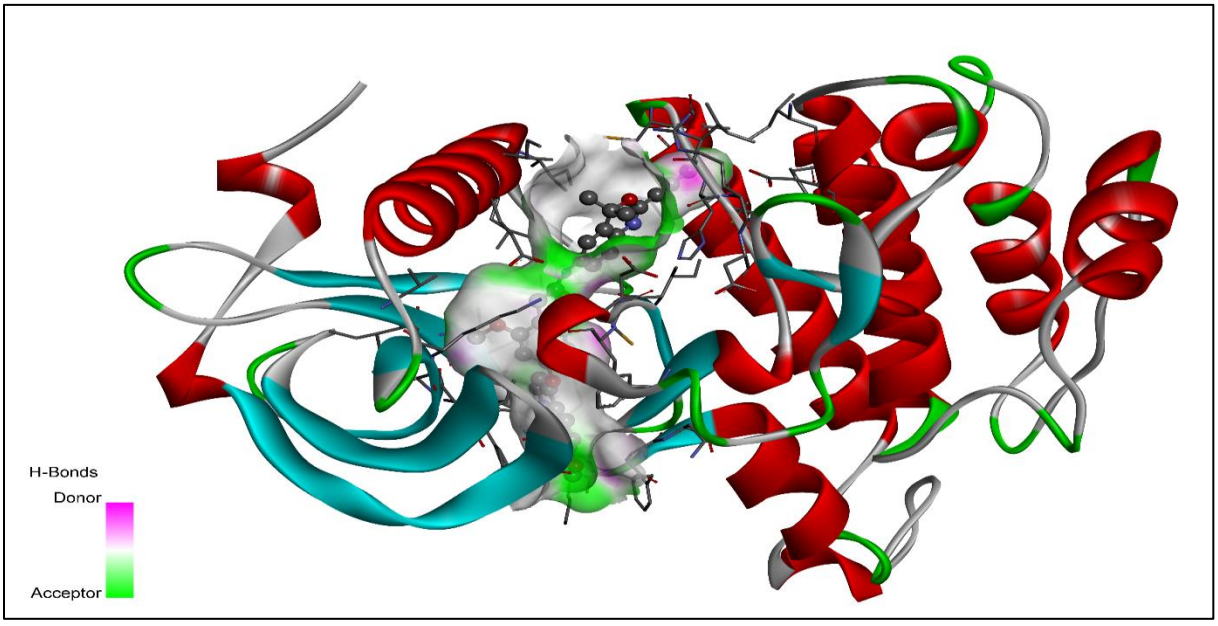

Figure 1. The 3D ribbon view of the enzyme with native ligand in the cavity

3. Results and Discussion

3.1 *In silico* ADMET Analysis

The primary reasons for drug failure can be attributed to a lack of effectiveness and safety. These factors are of utmost importance throughout the entire process of drug discovery and development, as the absorption, distribution, metabolism, excretion, and toxicity (ADMET) properties of chemicals significantly influence the outcomes. Table 1 presents a comprehensive compilation of the physicochemical properties exhibited by various molecules. In the context of physicochemical analysis, it is observed that the values of all the molecules under investigation fall within the acceptable range. The inclusion of logP and logS as components of the Lipinski rule of five was necessitated by the importance of the drug's lipophilicity. In the current study, it was observed that all the examined parameters fell within the acceptable range. Furthermore, these parameters exhibited optimal oral bioavailability, suggesting their potential for development as oral delivery agents[31,32].

The characteristics of the compounds that are indicative of their potential use as drugs are shown in Table 2. Calculations were made using a variety of factors, including QED, NPscore, Lipinski rule, Pfizer rule, GSK rule, Golden Triangle, and Chelator rule. The vast majority of the compounds exhibited a desirable range of quantitative estimate of drug-likeness (QED)[33,34]. The natural product-likeness score, commonly referred to as the NPscore, is typically observed to exhibit values within the -5 to 5 range. Based on the observed correlation, it can be inferred that a higher score is indicative of a heightened probability that the molecule under investigation belongs to the category of natural products (NPs)[35,36]. Both of the molecules exhibited properties similar to those of nanoparticles (NPs). Both of the compounds under investigation demonstrate adherence to the GSK rule and the Golden Triangle rule, suggesting the potential for a more advantageous ADMET (Absorption, Distribution, Metabolism, Excretion, and Toxicity) profile.

The absorption parameters of the molecules are presented in Table 3. The optimal Caco-2 permeability is observed when the value exceeds -5.15 Log unit. Regrettably, none of the molecules examined in this study exhibited the desired level of Caco-2 permeability[37]. The compound known as febrifugine has been found to exhibit activity as a substrate for P-glycoprotein (Pgp). Both of the molecules exhibited a level of inhibitory human intestinal absorption (HIA) that can be classified as moderate. The bioavailability of the molecules at F20% and F30% demonstrated values that fell within the acceptable range.

Table 4 presents a comprehensive depiction of the distribution and metabolism profile of molecules. The compound known as febrifugine exhibited a plasma protein binding (PPB) value of less than 90%, indicating a relatively low affinity for binding to plasma proteins. In contrast, glycosminine demonstrated a significantly higher PPB value of 96.52%, suggesting a strong propensity for binding to plasma proteins. The volume distribution (VD) of all the molecules in

the study fell within the acceptable range of 0.04-20L/kg, as determined by optimal conditions. Both of the molecules exhibited a moderate potential for penetrating the blood-brain barrier (BBB). The compound known as febrifugine has demonstrated the potential to inhibit cytochrome P450 enzymes (CYP)[15].

The tabulation of molecules' excretion and toxicity profile can be observed in Table 5. Both of the molecules demonstrated a moderate rate of clearance and displayed a relatively short half-life. The toxicity profile of the suggested molecules exhibited favorable properties, with a significant number of values falling within the acceptable range[15]. Table 6 presents a comprehensive overview of the environmental toxicity profile of various molecules, as indicated by their bioconcentration factors, IGC50 values, LC50FM values, and LC50DM values. The molecules exhibited an environmental toxicity profile that was found to be optimal and fell within the acceptable range.

Table 1. Physicochemical properties calculated for molecules

Code	Physicochemical Properties							
	Molecular Weight	Volume	nHA	nHD	nRot	TPSA	logS	logP
Febrifugine	301.140	303.165	6	2	4	84.220	-0.844	-0.057
Glycosminine	236.090	252.019	3	1	2	45.750	-3.245	2.447

Table 2. Drug-likeness properties of molecules

Code	Medicinal Chemistry						
	QED	NPscore	Lipinski Rule	Pfizer Rule	GSK Rule	Golden Triangle	Chelator Rule
Febrifugine	0.857	3.201	Accepted	Accepted	Accepted	Accepted	0
Glycosminine	0.743	-0.947	Accepted	Accepted	Accepted	Accepted	0

Table 3. An absorption parameters of molecules

Code	Absorption						
	Caco-2 Permeability	MDCK Permeability	Pgp-inhibitor	Pgp-substrate	HIA	F20%	F30%
Febrifugine	-5.634	6.3e-06	---	+++	--	++	+++
Glycosminine	-4.821	3.2e-05	---	---	---	+++	---

Table 4: Distribution and metabolism profile of molecules

Code	Distribution				Metabolism									
	PPB (%)	VD	BBB Penetration	Fu	CYP1A2		CYP2C19		CYP2C9		CYP2D6		CYP3A4	
					Inhibitor	Substrate	Inhibitor	Substrate	Inhibitor	Substrate	Inhibitor	Substrate	Inhibitor	Substrate
Febrifugine	23.928	1.811	+	81.587	---	---	---	--	---	--	---	--	---	--
Glycosminine	96.529	0.388	--	1.932	+++	+	+++	----	++	---	+	--	-	+

Table 5. Excretion and toxicity profile of molecules

Code	Excretion		Toxicity									
	CL	T1/2	H-HT	DILI	AMES Toxicity	Rat Oral Acute Toxicity	FDAMDD	Skin Sensitization	Carcinogencity	Eye Corrosion	Eye Irritation	Respiratory Toxicity
Febrifugine	7.176	0.780	++	+	--	-	+	-	-	---	---	-
Glycosminine	5.397	0.755	-	+++	-	-	--	--	--	---	--	++

Table 6. Environmental toxicity profile of molecules

Code	Environmental toxicity			
	Bioconcentration Factors	IGC50	LC50FM	LC50DM
Febrifugine	0.431	2.157	2.220	3.436
Glycosminine	0.615	3.239	3.963	5.142

3.2 Molecular Docking Studies

The computer technique known as molecular docking is used to conduct virtual screening of molecules, enabling the assessment of the preliminary activity potential of a ligand against certain biological targets. The attainment of this aim may be aided by assessing the ligand's affinity for binding to the particular target. The molecular docking interactions have been methodically documented and classified in Table 7. The table shown above offers a detailed summary of the many interactions that have been observed during the process of docking. Furthermore, Table 8 presents distinct docking configurations, providing tangible illustrations of

the molecular interactions. The binding affinities of the molecules have been compared with the binding mode of native ligand present in the crystal structure of VEGFR-2 kinase (PDB ID: 6XKV). Native ligand exhibited -8.7 kcal/mol of binding affinity and formed two conventional hydrogen bonds with Cys919. It also formed hydrophobic Interactions (Pi-sigma, Pi-Pi T-shaped, Alkyl, Pi-alkyl) with Leu840, His1026, Ile888, Cys1024, Leu889, Val848, Ala866, Cys919, Leu1035, and Cys1024. Febrifugine exhibited -8.8 kcal/mol of binding affinity and formed three conventional hydrogen bonds with Asp1046 and Cys919 and formed hydrophobic interactions (Pi-Sigma, Alkyl and Pi-Alkyl) with Leu840, Leu889, Val914, Val916 and Leu1035. Glycosminine showed -10 kcal/mol of binding affinity and formed one conventional and one Pi-donor hydrogen bonds with Cys919 and Phe1047. It also formed hydrophobic interactions (Pi-Sigma, and Pi-Alkyl) with Leu840, Val916, Leu1035, Val848, Ala866 and Lys868. From molecular docking it was observed that both the compounds formed more stable complex than native ligand. Both the compounds displayed formation of 2-3 conventional hydrogen bonds which indicates they has potential to modulate the activity of target enzyme. These compounds can be tested further using *in vitro* and *in vivo* models for VEGFR-2 kinase activity.

Table 7. The binding interactions of molecules with VEGFR-2 kinase

Active amino acid residues	Bond Length	Bond Type	Bond Category	Ligand energy	Docking score
NL					
CYS919	2.73884	Hydrogen Bond	Conventional Hydrogen Bond	933.34	-8.7
	3.06352				
LEU840	3.95706	Hydrophobic	Pi-Sigma		
HIS1026	5.40986		Pi-Pi T-shaped		
ILE888	4.13805		Alkyl		
CYS1024	3.8825				
LEU889	5.27859				
VAL848	5.45953		Pi-Alkyl		
ALA866	3.95797				
CYS919	5.0877				
LEU1035	4.42133				
CYS1024	5.44712				
HIS1026	5.28315				
Febrifugine					
ASP1046	2.21332	Hydrogen Bond	Conventional Hydrogen Bond	234.95	-8.8
	2.42381				
CYS919	2.15949				
LEU840	3.71459	Hydrophobic	Pi-Sigma		

LEU889	4.34113		Alkyl		
VAL899	5.22457				
VAL914	5.47123				
VAL916	4.41568				
LEU1035	5.32107		Pi-Alkyl		
Glycosminine					
CYS919	2.25791	Hydrogen Bond	Conventional Hydrogen Bond	173.5	-10
PHE1047	3.33834		Pi-Donor Hydrogen Bond		
LEU840	3.69883	Hydrophobic	Pi-Sigma		
VAL916	3.54094				
LEU1035	3.60011				
LEU840	5.46975		Pi-Alkyl		
VAL848	4.68218				
ALA866	3.8576				
ALA866	4.85434				
LEU1035	4.77733				
VAL848	4.74631				
ALA866	5.31329				
LYS868	4.25655				

Table 8. The docking poses of molecules

3D-docking poses	2D-docking poses
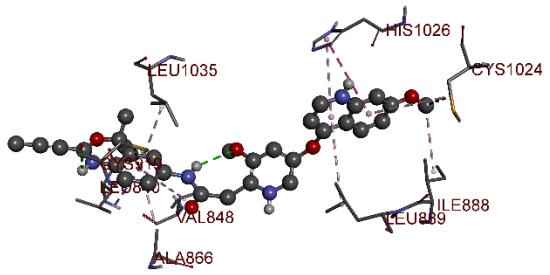	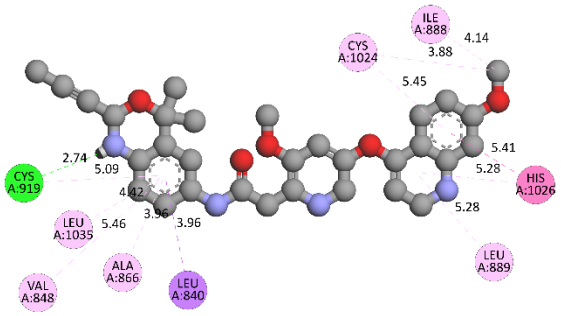
Native ligand	

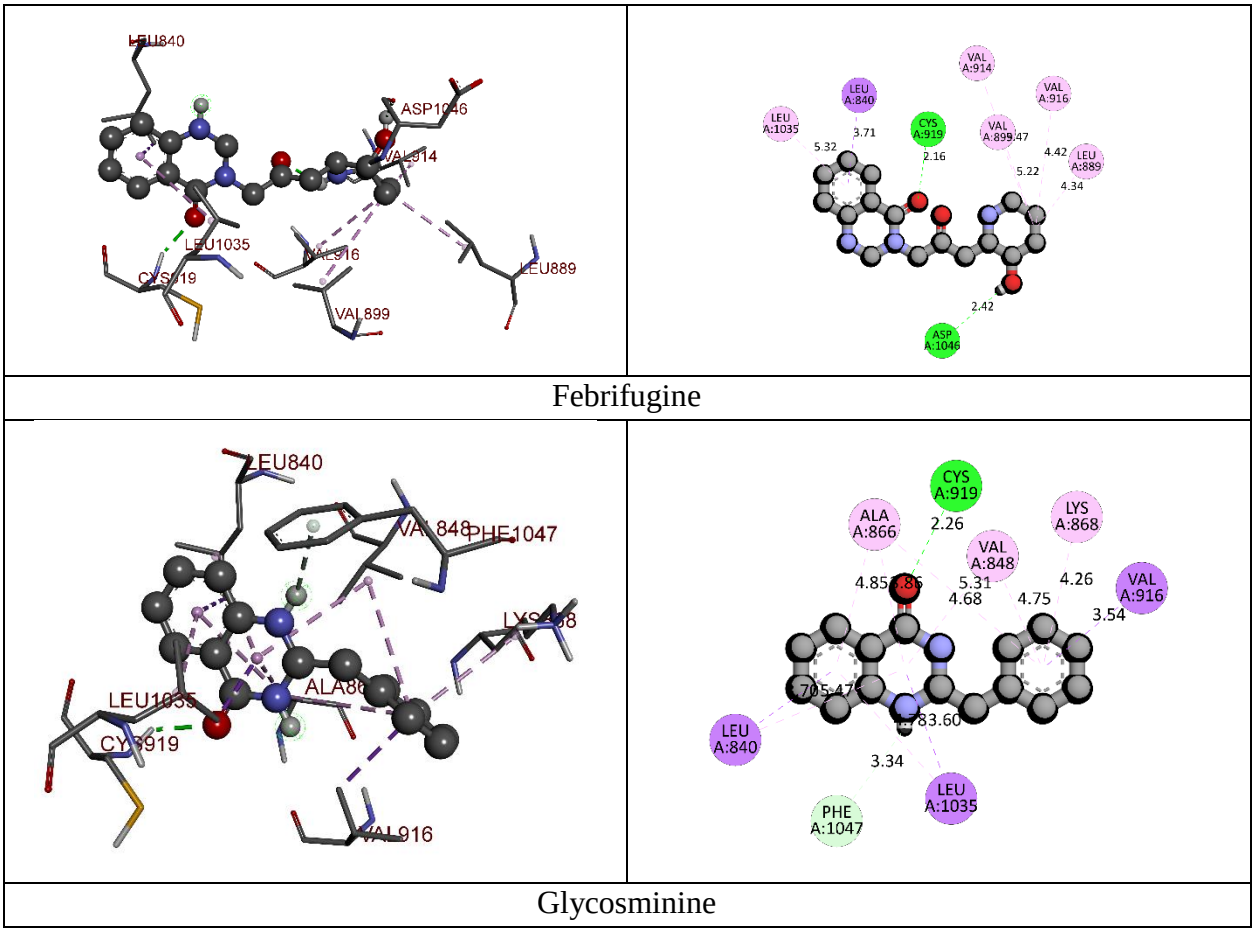

Conclusion

The quinazolinone alkaloids Febrifugine and Glycosminine were first identified in the Chinese plant Dichroa febrifuga. The inhibitors targeting Vascular Endothelial Growth Factor Receptor-2 (VEGFR-2) kinase have shown significant efficacy in inhibiting the processes of angiogenesis and lymphangiogenesis, therefore displaying noteworthy anti-cancer characteristics. In the present research, two naturally occurring chemicals, namely Febrifugine and Glycosminine, have been selected as the primary subjects of inquiry. The aim of this study is to evaluate the capacity of these compounds to serve as inhibitors of VEGFR-2 kinase activity. A comprehensive examination of the absorption, distribution, metabolism, excretion, and toxicity (ADMET) characteristics of these substances was conducted to evaluate their suitability as potential therapeutic candidates. Based on the in silico ADMET study, it was shown that these compounds exhibit very attractive drug-likeness features, hence indicating their potential as lead molecules for further molecular docking investigation. The results obtained from molecular docking analysis indicated that both compounds exhibited a higher degree of stability in complex formation compared to the native ligand. Both compounds exhibited the creation of 2-3

conventional hydrogen bonds, suggesting their ability to regulate the activity of the target enzyme. Further testing of these drugs may be conducted utilizing in vitro and in vivo models to assess their VEGFR-2 kinase activity.

References

(1) Mortlock, A.; Foote, K.; Kettle, J.; Aquila, B. *Kinase Inhibitors in Cancer*; Elsevier Inc., 2014. https://doi.org/10.1016/b978-0-12-409547-2.11033-9.

(2) Sánchez-Martínez, C.; Gelbert, L. M.; Lallena, M. J.; De Dios, A. Cyclin Dependent Kinase (CDK) Inhibitors as Anticancer Drugs. *Bioorganic Med. Chem. Lett.* **2015**, *25* (17), 3420–3435. https://doi.org/10.1016/j.bmcl.2015.05.100.

(3) Aziz, M. A.; Serya, R. A. T.; Lasheen, D. S.; Abouzid, K. A. M. Furo[2,3-d]Pyrimidine Based Derivatives as Kinase Inhibitors and Anticancer Agents. *Futur. J. Pharm. Sci.* **2016**, *2* (1), 1–8. https://doi.org/10.1016/j.fjps.2015.12.001.

(4) Ai, X.; Guo, X.; Wang, J.; Stancu, A. L.; Joslin, P. M. N.; Zhang, D.; Zhu, S. Targeted Therapies for Advanced Non-Small Cell Lung Cancer. *Oncotarget* **2018**, *9* (101), 37589–37607. https://doi.org/10.18632/oncotarget.26428.

(5) Arafa, R. K.; Nour, M. S.; El-Sayed, N. A. Novel Heterocyclic-Fused Pyrimidine Derivatives: Synthesis, Molecular Modeling and Pharmacological Screening. *Eur. J. Med. Chem.* **2013**, *69*, 498–507. https://doi.org/10.1016/j.ejmech.2013.08.042.

(6) Zhang, J.; Jiang, X.; Jiang, Y.; Guo, M.; Zhang, S.; Li, J.; He, J.; Liu, J.; Wang, J.; Ouyang, L. Recent Advances in the Development of Dual VEGFR and C-Met Small Molecule Inhibitors as Anticancer Drugs. *Eur. J. Med. Chem.* **2016**, *108*, 495–504. https://doi.org/10.1016/j.ejmech.2015.12.016.

(7) El-Helby, A. G. A.; Sakr, H.; Eissa, I. H.; Abulkhair, H.; Al-Karmalawy, A. A.; El-Adl, K. Design, Synthesis, Molecular Docking, and Anticancer Activity of Benzoxazole Derivatives as VEGFR-2 Inhibitors. *Arch. Pharm. (Weinheim).* **2019**, *352* (10). https://doi.org/10.1002/ardp.201900113.

(8) Zhang, Y.; Zhang, M.; Wang, Y.; Fan, Y.; Chen, X.; Yang, Y.; Hua, Y.; Xie, W.; Lu, T.; Tang, W.; Chen, Y.; Liu, H. Protein–Ligand Interaction-Guided Discovery of Novel VEGFR-2 Inhibitors. *J. Biomol. Struct. Dyn.* **2020**, *38* (9), 2559–2574. https://doi.org/10.1080/07391102.2019.1635915.

(9) Smullen, S.; McLaughlin, N. P.; Evans, P. Chemical Synthesis of Febrifugine and Analogues. *Bioorganic Med. Chem.* **2018**, *26* (9), 2199–2220. https://doi.org/10.1016/j.bmc.2018.04.027.

(10) Mitsui, Y.; Miura, M.; Kato, K. In Vitro Effects of Febrifugine on Schistosoma Mansoni Adult Worms. *Trop. Med. Health* **2020**, *48* (1). https://doi.org/10.1186/s41182-020-00230-x.

(11) Zhang, S.; Wang, Y.; Cai, J.; Liu, D.; Yan, Y.; Zhang, H.; Li, L.; Wang, X.; Xiang, W.; Zhang, J. Discovery of Febrifugine with Specific Anti-Phytophthora Oomycete Activity

Isolated from Dichroa Febrifuga Lour. *Ind. Crops Prod.* **2022**, *178*. https://doi.org/10.1016/j.indcrop.2022.114651.

(12) Kim, S.; Chen, J.; Cheng, T.; Gindulyte, A.; He, J.; He, S.; Li, Q.; Shoemaker, B. A.; Thiessen, P. A.; Yu, B.; Zaslavsky, L.; Zhang, J.; Bolton, E. E. PubChem in 2021: New Data Content and Improved Web Interfaces. *Nucleic Acids Res.* **2021**, *49* (D1), D1388–D1395. https://doi.org/10.1093/nar/gkaa971.

(13) Molinspiration Cheminformatics. *Choice Rev. Online* **2006**, *43* (11), 43-6538-43–6538. https://doi.org/10.5860/choice.43-6538.

(14) Daina, A.; Michielin, O.; Zoete, V. SwissADME: A Free Web Tool to Evaluate Pharmacokinetics, Drug-Likeness and Medicinal Chemistry Friendliness of Small Molecules. *Sci. Rep.* **2017**, *7*. https://doi.org/10.1038/srep42717.

(15) Xiong, G.; Wu, Z.; Yi, J.; Fu, L.; Yang, Z.; Hsieh, C.; Yin, M.; Zeng, X.; Wu, C.; Lu, A.; Chen, X.; Hou, T.; Cao, D. ADMETlab 2.0: An Integrated Online Platform for Accurate and Comprehensive Predictions of ADMET Properties. *Nucleic Acids Res.* **2021**, *49* (W1), W5–W14. https://doi.org/10.1093/nar/gkab255.

(16) Panneerselvam, S.; Yesudhas, D.; Durai, P.; Anwar, M. A.; Gosu, V.; Choi, S. A Combined Molecular Docking/Dynamics Approach to Probe the Binding Mode of Cancer Drugs with Cytochrome P450 3A4. *Molecules* **2015**, *20* (8), 14915–14935. https://doi.org/10.3390/molecules200814915.

(17) Pagadala, N. S.; Syed, K.; Tuszynski, J. Software for Molecular Docking: A Review. *Biophys. Rev.* **2017**, *9* (2), 91–102. https://doi.org/10.1007/s12551-016-0247-1.

(18) Diller, D. J.; Merz, K. M. High Throughput Docking for Library Design and Library Prioritization. *Proteins Struct. Funct. Genet.* **2001**, *43* (2), 113–124. https://doi.org/10.1002/1097-0134(20010501)43:2<113::AID-PROT1023>3.0.CO;2-T.

(19) Morris, G. M.; Lim-Wilby, M. Molecular Docking. *Methods Mol. Biol.* **2008**, *443*, 365–382. https://doi.org/10.1007/978-1-59745-177-2_19.

(20) Dar, A. M.; Mir, S. Molecular Docking: Approaches, Types, Applications and Basic Challenges. *J. Anal. Bioanal. Tech.* **2017**, *08* (02). https://doi.org/10.4172/2155-9872.1000356.

(21) Dallakyan, S.; Olson, A. J. Small-Molecule Library Screening by Docking with PyRx. *Methods Mol. Biol.* **2015**, *1263* (1263), 243–250. https://doi.org/10.1007/978-1-4939-2269-7_19.

(22) Rappé, A. K.; Casewit, C. J.; Colwell, K. S.; Goddard, W. A.; Skiff, W. M. UFF, a Full Periodic Table Force Field for Molecular Mechanics and Molecular Dynamics Simulations. *J. Am. Chem. Soc.* **1992**, *114* (25), 10024–10035. https://doi.org/10.1021/ja00051a040.

(23) San Diego: Accelrys Software Inc. Discovery Studio Modeling Environment, Release 3.5. *Accelrys Softw. Inc.* **2012**.

(24) Khan, S. L.; Siddiqui, F. A.; Jain, S. P.; Sonwane, G. M. Discovery of Potential Inhibitors

of SARS-CoV-2 (COVID-19) Main Protease (Mpro) from Nigella Sativa (Black Seed) by Molecular Docking Study. *Coronaviruses* **2020**, *2* (3), 384–402. https://doi.org/10.2174/2666796701999200921094103.

(25) Chaudhari, R. N.; Khan, S. L.; Chaudhary, R. S.; Jain, S. P.; Siddiqui, F. A. B-Sitosterol: Isolation from Muntingia Calabura Linn Bark Extract, Structural Elucidation And Molecular Docking Studies As Potential Inhibitor of SARS-CoV-2 Mpro (COVID-19). *Asian J. Pharm. Clin. Res.* **2020**, *13* (5), 204–209. https://doi.org/10.22159/ajpcr.2020.v13i5.37909.

(26) Khan, S. L.; Siddiqui, F. A.; Shaikh, M. S.; Nema, N. V.; Shaikh, A. A. Discovery of Potential Inhibitors of the Receptor-Binding Domain (RBD) of Pandemic Disease-Causing SARS-CoV-2 Spike Glycoprotein from Triphala through Molecular Docking. *Curr. Chinese Chem.* **2021**, *01*. https://doi.org/10.2174/2666001601666210322121802.

(27) Khan, S. L.; Sonwane, G. M.; Siddiqui, F. A.; Jain, S. P.; Kale, M. A.; Borkar, V. S. Discovery of Naturally Occurring Flavonoids as Human Cytochrome P450 (CYP3A4) Inhibitors with the Aid of Computational Chemistry. *Indo Glob. J. Pharm. Sci.* **2020**, *10* (04), 58–69. https://doi.org/10.35652/igjps.2020.10409.

(28) Siddiqui, F. A.; Khan, S. L.; Marathe, R. P.; Nema, N. V. Design, Synthesis, and In Silico Studies of Novel N-(2-Aminophenyl)-2,3- Diphenylquinoxaline-6-Sulfonamide Derivatives Targeting Receptor- Binding Domain (RBD) of SARS-CoV-2 Spike Glycoprotein and Their Evaluation as Antimicrobial and Antimalarial Agents. *Lett. Drug Des. Discov.* **2021**, *18* (9), 915–931. https://doi.org/10.2174/1570180818666210427095203.

(29) Shntaif, A. H.; Khan, S.; Tapadiya, G.; Chettupalli, A.; Saboo, S.; Shaikh, M. S.; Siddiqui, F.; Amara, R. R. Rational Drug Design, Synthesis, and Biological Evaluation of Novel N-(2-Arylaminophenyl)-2,3-Diphenylquinoxaline-6-Sulfonamides as Potential Antimalarial, Antifungal, and Antibacterial Agents. *Digit. Chinese Med.* **2021**, *4* (4), 290–304. https://doi.org/10.1016/j.dcmed.2021.12.004.

(30) Khan, S.; Kale, M.; Siddiqui, F.; Nema, N. Novel Pyrimidine-Benzimidazole Hybrids with Antibacterial and Antifungal Properties and Potential Inhibition of SARS-CoV-2 Main Protease and Spike Glycoprotein. *Digit. Chinese Med.* **2021**, *4* (2), 102–119. https://doi.org/10.1016/j.dcmed.2021.06.004.

(31) Waring, M. J. Lipophilicity in Drug Discovery. *Expert Opin. Drug Discov.* **2010**, *5* (3), 235–248. https://doi.org/10.1517/17460441003605098.

(32) Lobo, S. Is There Enough Focus on Lipophilicity in Drug Discovery? *Expert Opin. Drug Discov.* **2020**, *15* (3), 261–263. https://doi.org/10.1080/17460441.2020.1691995.

(33) Bickerton, G. R.; Paolini, G. V.; Besnard, J.; Muresan, S.; Hopkins, A. L. Quantifying the Chemical Beauty of Drugs. *Nat. Chem.* **2012**, *4* (2), 90–98. https://doi.org/10.1038/nchem.1243.

(34) Kosugi, T.; Ohue, M. Quantitative Estimate Index for Early-Stage Screening of

Compounds Targeting Protein-Protein Interactions. *Int. J. Mol. Sci.* **2021**, *22* (20). https://doi.org/10.3390/ijms222010925.

(35) Ertl, P.; Roggo, S.; Schuffenhauer, A. Natural Product-Likeness Score and Its Applications in the Drug Discovery Process. *Chem. Cent. J.* **2008**, *2* (S1). https://doi.org/10.1186/1752-153x-2-s1-s2.

(36) Menke, J.; Massa, J.; Koch, O. Natural Product Scores and Fingerprints Extracted from Artificial Neural Networks. *Comput. Struct. Biotechnol. J.* **2021**, *19*, 4593–4602. https://doi.org/10.1016/j.csbj.2021.07.032.

(37) Lee, J. B.; Zgair, A.; Taha, D. A.; Zang, X.; Kagan, L.; Kim, T. H.; Kim, M. G.; Yun, H. yeol; Fischer, P. M.; Gershkovich, P. Quantitative Analysis of Lab-to-Lab Variability in Caco-2 Permeability Assays. *Eur. J. Pharm. Biopharm.* **2017**, *114*, 38–42. https://doi.org/10.1016/j.ejpb.2016.12.027.